EXTINCTION AND SCATTERING OF MILLIMETER WAVES BY CLOUD AND PRECIPITATION PARTICLES

V.F. Terzi, A.G. Konyukhov, F.S. Yakupova, and L.V. Kurt

State Institute of Applied Optics, Kazan'
Received August 14, 1991

This paper is devoted to computer simulations of the optical characteristics of different polydisperse systems of spherical particles relevant to represent various forms of clouds and precipitation (rain, snow, and hail) in the spectral region from 0.5 to 10 mm. The calculation are made using the Mie theory formulas.[8,10] *The microstructure parameters and optical constants of the particulate matter are used as the input parameters for stimulations.*

The methods of microwave remote sounding of atmospheric water vapor content from space[1,2] and underlying surface[3,4] have attained wide use today. This necessitates a more accurate determination of the optical characteristics (OC) of the atmosphere in the millimeter spectral range including the absorption by molecular components[5–7] as wel1 as extinction and scattering on the disperse component[7–9] of the atmosphere.

This paper deals with computer simulation of optical characteristics (spectral coefficients of extinction and scattering, and scattering matrix for different polydisperse systems of spherical particles describing different forms of clouds and precipitation (rain, snow, and hail) in the spectral range of from 0.5 to 10 mm.

MICROSTRUCTURE OF CLOUDS AND PRECIPITATION

To describe the particle size distribution function $n(r)$ different analytical expressions[8,9] are used, most common of which are:

1) the Laws–Parsons distribution[8]

$$n(r) = \frac{10^3}{4.8\pi}\frac{RM(r)}{r^3V(r)}, \qquad (1)$$

where R is the rain intensity (mm/hr), V is the speed of rain drops at the ground surface (m/s), r is the particle radius (mm), and $M(r)$ is the volume percentage of water determined from tabulated experimental data;

2) the Marshall–Palmer distribution[9]

$$n(r) = 1.6\cdot 10^4 \exp\,(-8.2\,R^{-0.21}\cdot r), \qquad (2)$$

3) the modified Deirmendjian gamma–distribution

$$n(r) = A\,r^a \exp\,(-b\,r^c), \qquad (3)$$

where the microstructure parameters a, b, and c and the normalizing factor A for different cloud forms and precipitation are listed in Table I. Theoretical values of modal particle radius r_m (at which the distribution $n(r)$ takes its maximum value), a number density of particles N, water content W, and the extinction coefficient σ_a at the wavelength 0.55 μm calculated using the Mie theory formulas are also given in this table.

TABLE I. Reference models used in calculating millimetre wave attenuation and scattering by clouds and precipitation.

Shape of clouds and models of precipitation	Parameters of microstructure						Water content	Extinction coefficient
	a	b	c	r_m(μm)	N(cm^{-3})	A	W, (g/m^3)	σ_s, km^{-1}
Stratus	5	0.939	1.05	4.70	10^2	9.792(–1)	0.114	23.78
Stratocumulus	5	0.576	1.19	5.33	10^2	2.823(–1)	0.141	28.40
Heavy cumulus	4	0.667	1.00	6.00	10^2	0.548	0.297	44.20
Nimbostratus	5	0.402	1.24	6.61	10^2	8.061(–1)	0.235	37.03
High sheet clouds	2	0.0027	2.46	10.19	10^2	1.978(–1)	0.796	88.71
Cumulo-nimbus clouds	1	0.0017	2.41	9.67	10^2	1.097	1.034	100.30
Model c.6	2	0.100	1.00	20.0	10^{-1}	0.500(–4)	0.025	0.67
Rain–4	2	0.057	0.50	70.0	10^{-3}	0.497(–7)	0.117	0.366
Rain–10	4	0.012	1.00	333.0	10^{-3}	1.033(–14)	0.509	1.32
Rain–50	6	0.010	1.00	600.0	10^{-3}	1.383(–20)	2.110	3.54

Note: The model C.6 relates to a water fraction of rail fall, the models Rain–4, Rain–10, and Rain–50 relate to precipitation with rates 4, 10, and 50 mm/hr. The data, e.g., 9.792(–1) relates to $9.792\cdot 10^{-1}$.

In the region of large particle size and intensity of a rain of 4, 10, and 50 mm/h all this distribution functions agree quite well, provided that relevant values of the parameters a, b, and c are taken from Table I.

0235-6880/92/02 136-04 $02.00

OPTICAL CONSTANTS FOR WATER, ICE, AND SNOW

The optical constant $m = n - i\kappa$ for water and ice were calculated using the formulas from Ref. 11 and are shown in Figs. 1 and 2 for two temperatures + 20 and – 20°C. As can be seen from Fig. 1, real part n of the refractive index for ice remains unchanged over the whole spectral region from 0.5 to 100 mm and is equal to 1.78, while for water it increases almost by a factor of 5. An imaginary part of the index of refraction for water reaches maximum at λ = 10 mm, and κ for ice it is four orders of magnitude lower.

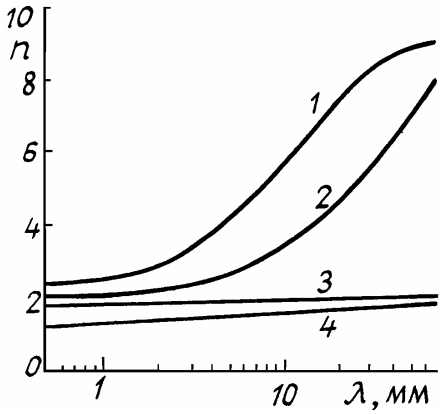

FIG. 1. Spectral dependence o[the real part of the index of refraction in a millimeter range: curve 1) n_w and T = –20°C, 2) n_w and T = 20°C, 3) n_i and T = –20°C, 4) n_s and T = – 20°C (W = 7%)

Recent experimental studies of the dielectric constant of water in the millimeter spectral range ($m = \sqrt{\varepsilon}$) are discussed in Ref. 14. Some new data on the Debye dielectric constant ε_∞ being equal to 4.93, 4.86, 4.73, and 4.72 for T = 283, 293, 303 and 313 K, respectively, are also presented in Ref. 14. The calculation of ε and m made using the formulas from Ref. 11 for these values of ε_∞ are in a poor agreement with the data obtained for $\varepsilon = \varepsilon' - i\varepsilon''$ in Ref. 14 than the data taken from Ref. 11, i.e., 5.356, 5.179, 4.74, and 4.038 for the same temperatures (see Table II).

Optical constants for snow are calculated using the analytical expressions[12] with account of water, ice and air mixture. The formula used for calculating the dielectric constant of snow ε_s is

$$\frac{\varepsilon_s - 1}{\varepsilon_s + U} = W\frac{\varepsilon_w - 1}{\varepsilon_w + U} + \frac{\sqrt{W} - W}{0.92}\frac{\varepsilon_i - 1}{\varepsilon_i + U}, \qquad (4)$$

where ε_w and ε_i; are the dielectric constants of water and ice, W is the snow humidity, and U is the factor whose value depends on crystal shape and orientation in snowflakes. According to Ref. 14, we have for a dry snow $0 < W < 0.05$ and $U = 2$, for a humid snow $0.3 < W < 3$ and $U = 8$, for a wet snow $5 < W < 10$ and $U = 20$, and for slush $15 < W < 30$ and $U = \infty$. The optical constants n and κ for snow calculated by formula (4) at W = 7% and $U = 20$ are also shown in Figs. 1 and 2. The value n is weakly varying in the spectral range of from 0.5 to 100 mm for a humid snow, and κ_s follows the behavior of κ_w with the absolute value which is an order of magnitude smaller.

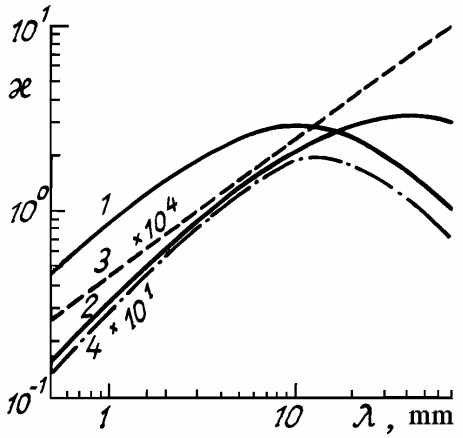

FIG. 2. Spectral dependence of the imaginary part of the refractive index for water, ice, and snow (see notation in Fig. 1).

TABLE II. Optical constants for water at different temperature.

T	Wave frequency, cm^{-1}	Ref. 14			n	ε′	ε″
		n	ε′	ε″			
283K	5.86	2.72	5.71	7.10	2.62	5.76	5.51
	6.84	2.61	5.41	6.24	2.55	5.65	4.72
	7.81	2.56	5.35	5.57	2.50	5.58	4.14
	8.79	2.50	5.29	4.95	2.47	5.54	3.68
	9.77	2.46	5.21	4.44	2.44	5.50	3.32
	10.74	2.42	5.15	4.14	2.42	5.48	3.02
	11.72	2.38	5.05	3.78	2.41	5.46	2.77
	12.70	2.36	5.02	3.46	2.39	5.45	2.55
	13.67	2.33	4.86	3.57	2.38	5.43	2.37
303K	5.86	2.94	6.28	8.99	2.89	5.96	8.99
	6.84	2.82	5.85	8.16	2.76	5.65	7.75
	7.81	2.65	5.55	6.37	2.66	5.45	6.81
	8.79	2.62	5.36	6.43	2.59	5.31	6.07
	9.77	2.53	5.21	5.54	2.53	5.20	5.47
	10.74	2.49	5.16	5.05	2.48	5.13	4.98
	11.72	2.46	5.12	4.72	2.44	5.07	4.57
	12.70	2.43	5.13	4.28	2.41	5.02	4.22
	13.67	2.43	5.25	3.97	2.38	4.99	3.93

OPTICAL CHARACTERISTICS OF CLOUDS AND PRECIPITATION

In the optical and radiowave ranges different definitions of the atmospheric transmission function are used, i.e.,

$$\tau_{opt} = \exp(-\sigma_a z), \quad \tau_{rad} = 10^{-\sigma'_a z}, \qquad (5)$$

where $\sigma_a z$ is the optical thickness, σ_a is the extinction coefficient (km^{-1}), z is the distance along the observation path, $\sigma'_a z$ is the attenuation of radiation by the atmospheric layer z (dB) and, σ'_a is the extinction coefficient (dB/km). Below we use only the first definition from functions (5), the transition to σ'_a is accomplished, according to (5), in a rather simple way $\sigma'_a = 0.4343\ \sigma_a$.

Shown in Figs. 3 and 4 are the results of the Mie theory calculations of spectral extinction coefficients σ_a for different cloud forms, rains, snow, and ice.

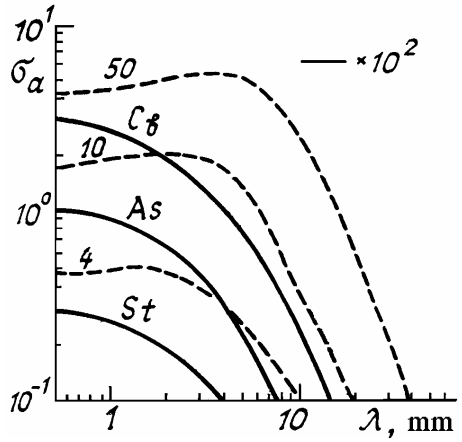

FIG. 3. Spectral dependence of the extinction coefficient of clouds Cb, As, *and* St *(curves are risen by two orders of magnitude) and the related rain models* 4, 10, *and* 50 *(microstructure in Table I).*

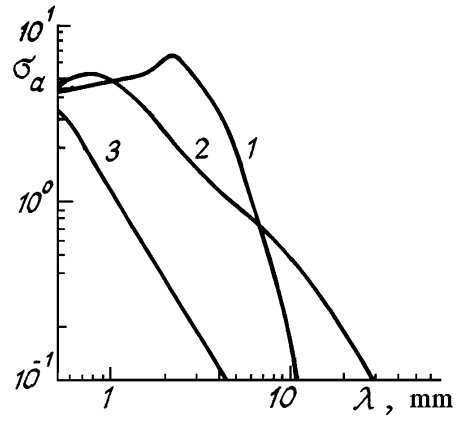

FIG. 4. Spectral dependence of the extinction coefficient: 1) ice–50, 2) *snow–50 (W=7%). and 3) snow–50 (W* = 1%).

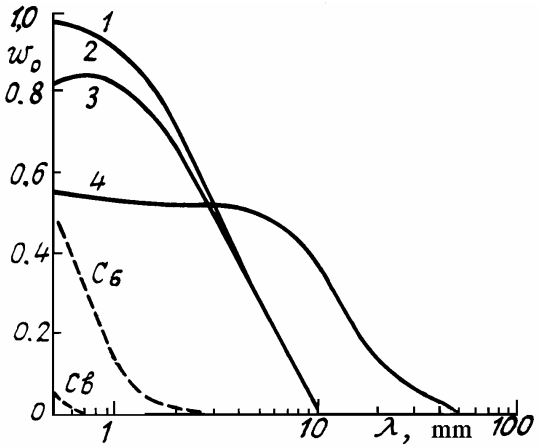

FIG. 5. Spectral dependence of probability of photon survival: 1) ice–50, 2) snow–50 (W=1%), 3) now–50 (W=7%), and 4) rain–50.

It can be easily seen that the attenuation by clouds is by two orders of magnitude weaker than that by precipitation. The clouds primarily absorb a millimeter–wave radiation since the probability of photon survival ω_0 (see Fig. 5) is very low $\omega_0 = \frac{\sigma_a^p}{\sigma_a}$, where σ_a^p is the spectral coefficient of scattering). The absolute value of σ_a for clouds is of the order of 10^{-2} km^{-1} what corresponds to the meteorological visual range $V = 3.91/\sigma_a$ of more than 100 km. Visual range for rains (depending on raindrop size) is of the order of (1–05) km which in the visible range corresponds to a slight fog with sufficiently strong absorption (see ω_0 in Fig. 5). The value S_a sharply decreases with wavelength ($\lambda > 5$ mm) in all models of rain. Spectral behaviors of σ_a of the largest particles of a scattering ensemble are shown in Fig. 4. It can be seen from this figure that although σ_a for ice at $\lambda < 2$ mm is higher than that for water (Fig. 3), σ_a for ice and snow sharply decreases at λ larger than 2 mm, ω_0 for snow being much higher than ω_0 for rain at $\lambda < 3$ mm and lower at $\lambda > 3$ mm. Because of small values of κ_1 the probabi1ity of photon survival for ice is very close to unity what results in pure scattering of millimeter waves in ice crystal clouds or hail.

One more important feature of light scattering on particles is the scattering phase function f which describes the angular distribution of scattered radiation. Figures 6 and 7 show some scattering phase functions (at $\lambda = 0.5$ and 2 mm) normalized using the relation

$$\int_{\Omega} f(Q)\mathrm{d}\Omega = \omega_0, \qquad (6)$$

where the integration is carried out over the entire sphere. Taking into account the fact that $f(Q)$ for spherical particles is not a function of azimuth angle and is symmetric with respect to W,

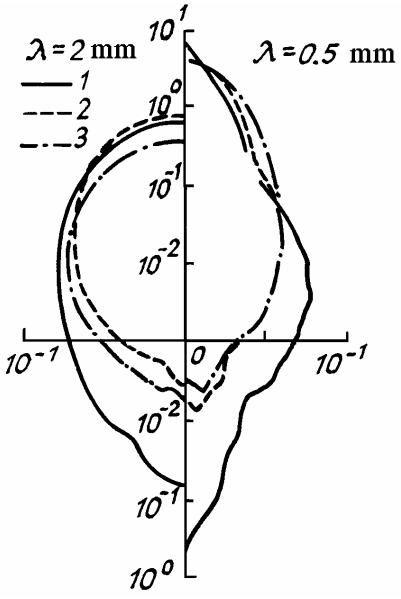

FIG. 6. Scattering phase functions at two wavelengths: 1) *rain–4, 2) rain–10, and 3) rain–50.*

Figs. 6 and 7 show $f(Q)$ for the scattering angles of 0° (upward) to 180° (downward). As can be seen from Fig. 6, the fraction of largest particles possesses the highest forward peak in the scattering phase function,

while the fraction of small particles greatly contributes to the backscatter. Similar pattern is observed in Fig. 7 for the models snow–10 and snow–50, with the maximum of scattering (most pronounced at $\lambda = 0.5$ mm) at the scattering angles of $Q \sim 160–170°$ due to the glory effect. Quite different pattern for backscattering is observed for ice particles: the scattering phase function increases by more than one order of magnitude compared with that for models of rain and snow.

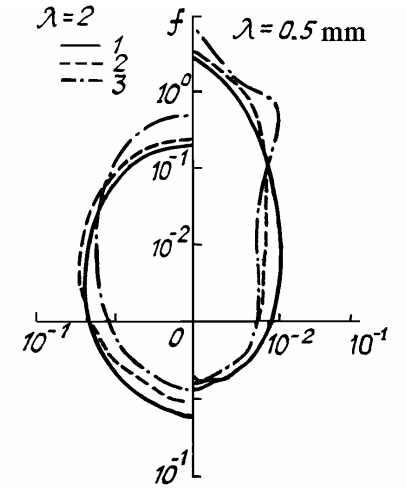

FIG. 7. Scattering phase functions at two wavelengths: 1) ice–50, 2) snow–50 (W = 7%), and 3) snow–10 (W = 7%).

The shapes of particles greatly affect the shape the scattering phase function[13] though the calculational results given in Ref. 9 with insignificant deviation of a particle shape from a spherical one show that the extinction coefficient and the scattering phase function only slightly differ from analogous values for spherical particles.

REFERENCES

1. K.Ya. Kondrat'ev and V.V. Melent'ev, *Spaceborne Remote Sensing of Clouds and Water Content of the Atmosphere* (Gidrometeoizdat, Leningrad, 1987), 263 pp.
2. *Electromagnetic waves in the Atmosphere and in Space* (Nauka, Moscow, 1986), 272 pp.
3. S.A. Zhevakin, Izv. Vyssh. Uchebn. Zaved., Ser. Radiofiz. **21**, No. 8, 1122–1131 (1978).
4. V.S. Kostsov and Yu.M. Timofeev, *ibid*. **31**, No. 5, 519–527 (1988).
5. S.A. Zhevakin and A.P. Naumov, *ibid*. **9**, 433–450 (1966).
6. S.A. Zhevakin and A.P. Naumov, *ibid*. **10**, No. 10, 1213–1243 (1967).
7. A.V. Sokolov and E.V. Sukhonin, *Millimeter Wave Attenuation in the Atmosphere,* VINITI "Radiotekhnika" **20**, 109–205 (1980).
8. V.I. Rozenberg, *Electromagnetic Waves Scattering and Attenuation by Atmospheric Particles* (Gidrometeoizdat, Leningrad, 1972), 348 pp.
9. T. Oguti, Proc. IEEE **71**, No. 9, 6–65 (1983).
10. D. Deirmendjian, *Electromagnetic Scattering on Spherical Polydispersions* (Elsevier, Amsterdam, American Elsevier, New York, 1969).
11. P.S. Ray, Appl. Opt. **11**, No. 8,1836–1844 (1972).
12. M.N.O. Sadiku, Appl. Opt. **24**, No. 4, 572–575 (1985).
13. A. Mugnai and W.J. Wiscombe, J. Atm. Sci. **37**, No. 6, 1291 (1980).
14. J.B. Hasted, S.K. Husain, F.A.M. Frescura, and J.R. Birch, Infrared Phys. **27**, No. 1, 11 (1987).